Inorganic Chemistry

Article

pubs.acs.org/IC

A Nanosized {Ag@Ag_{12}} "Molecular Windmill" Templated by Polyoxometalates Anions

Lei Wang,[†] Weiting Yang,[†] Wei Zhu,[†] Xingang Guan,[‡] Zhigang Xie,*[,‡] and Zhong-Ming Sun*[,†]

[†]State Key Laboratory of Rare Earth Resource Utilization and [‡]State Key Laboratory of Polymer Physics and Chemistry, Changchun Institute of Applied Chemistry, Chinese Academy of Sciences, 5625 Renmin Street, Changchun, Jilin 130022, China

Supporting Information

ABSTRACT: Reaction of multidentate 5-(4-imidazol-1-yl-phenyl)-2*H*-tetrazole (**L**) ligand with Ag(I) ions in the existence of $H_3PW_{12}O_{40}$ as anionic template under hydrothermal conditions results in tridecanuclear silver cluster–polyoxometalates hybrid: $\{Ag_{13}L_{12}\}\{PW_{12}O_{40}\}_4\cdot 30H_2O$ (**1**). X-ray single crystal diffraction analysis indicates that the main structural feature of **1** is a nanosized molecular windmill-shaped polynuclear Ag cluster with intriguing $\{M@M_{12}\}$-type cuboctahedral topology. The as-synthesized compound exhibits effective photocatalytic activity in the photodegradation of Rhodamine-B (RhB) and antibacterial activity against *Escherichia coli*, respectively.

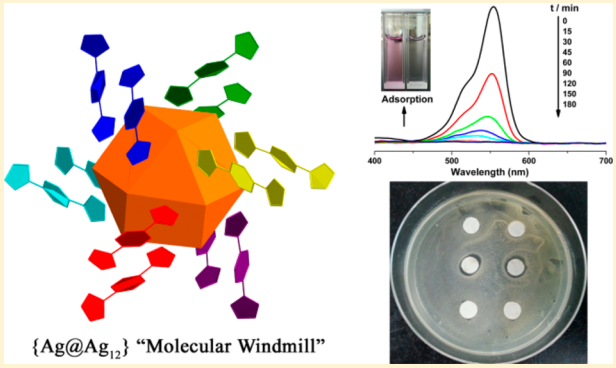

INTRODUCTION

Owing to the fascinating topologies and potential development of new functional materials, construction of polynuclear metal complexes currently remains one of the most active research frontiers. With regard to polynuclear silver(I) complexes, the continuous motivations are driven not only by their rich coordination chemistry but also by their extensive applications in luminescence, catalysis, pharmaceutical field, etc.[1] During the past decades, a large number of polynuclear silver(I) complexes have been prepared with intriguing geometric shapes ranging from simple triangles, discrete metallamacrocycles, dense lamellar structures, and spacious cages to more complicated giant clusters.[2] However, in contrast to the sophistication of the silver alkynyl clusters and silver chalcogenide clusters,[1a] the nitrogen-donor multidentate ligand-supported clusters are far less developed, in particular for those with high symmetry and high-nuclear geometries.[2b,d,3]

On the other hand, some anions (halogen, CrO_4^{2-}, SO_4^{2-}, etc.) usually play an essential structure-directing role in the syntheses of polynuclear silver(I) complexes.[4] In contrast with those simple anions mentioned above, polyoxometalates (POMs)[5] as unique molecular anionic oxide clusters with controllable geometric structures, high negative charges, and excellent physicochemistry properties have been evidenced as effective templates and charge compensators by Gao and Mak et al. for the preparation of high-nuclearity silver(I) alkynyl clusters.[6] There have been few examples of POMs templated polynuclear silver clusters supported by multidentate nitrogen ligands, such as bizole, tetrazole, and their derivatives; examples of higher nuclearity and order clusters are very rare. Known examples include a double calix[3]arene shaped hexamer with $\{PMo_{12}O_{40}\}^{3-}$ template,[7a] and keggin anion templated chairlike heptanuclear supported by benzotriazolate ligands.[7b]

In this article, a multidentate 5-(4-imidazol-1-yl-phenyl)-2*H*-tetrazole (**L**) ligand containing both imidazole and tetrazole functions was introduced in the synthesis of high-nuclearity silver cluster by using the "POMs anions directing approach". Reaction of **L** with Ag(I) ions in the presence of $H_3PW_{12}O_{40}$ under hydrothermal conditions produced a tridecanuclear silver cluster–POMs hybrid: $\{Ag_{13}L_{12}\}\{PW_{12}O_{40}\}_4\cdot 30H_2O$ (**1**). This compound features the molecular windmill-shaped polynuclear silver cluster supported by multidentate nitrogen ligands and using POMs as templates. Its photocatalytic and antibacterial activities were also investigated.

EXPERIMENTAL SECTION

General Procedures and Instrumentations. The $H_3PW_{12}O_{40}\cdot xH_2O$ was received from the Sinopharm Chemical Reagent Corporation Ltd. The ligand 5-(4-imidazol-1-yl-phenyl)-2*H*-tetrazole (**L**) was purchased from Jinan Henghua Company. Other chemicals used during this investigation were reagent grade and used as received. Elemental analyses of C, H, and N were examined with a VarioEL analyzer. Powder X-ray diffraction (XRD) data were collected on a D8 Focus (Bruker) diffractometer at 40 kV and 30 mA with monochromated Cu Kα radiation (λ = 1.5405 Å). Thermogravimetric analysis (TGA) was recorded on a Thermal Analysis Instrument (SDT 2960, TA Instruments, New Castle, DE) from room temperature to 900 °C under air atmosphere with a heating rate of 10 °C/min. The infrared (IR) spectrum was measured within the 650–4000 cm^{-1} region on a Nicolet iS10 spectrometer with ITR mode. The liquid

Received: July 11, 2014
Published: October 14, 2014

   dx.doi.org/10.1021/ic501657p | *Inorg. Chem.* 2014, 53, 11584–11588

UV−vis absorption spectra were recorded on a 756 CRT UV−vis spectrophotometer.

Synthesis of $\{Ag_{13}(L)_{12}\}\{PW_{12}O_{40}\}_4\cdot 30H_2O$ (1). A mixture of $H_3PW_{12}O_{40}\cdot xH_2O$ (0.3 g, 0.1 mmol), $AgNO_3$ (117 mg, 0.68 mmol), **L** ligand (0.063 g, 0.3 mmol), and 10 mL of water was stirred for ∼60 min. The resulting milky white solution was transferred to a 20 mL Teflon-lined autoclave carefully and kept under autogenous pressure at 150 °C for 5 d. After the solution slowly cooled to room temperature, yellow block crystals of **1** were separated manually from the colorless impurity, washed with distilled water, and dried at room temperature for the further characterization. Anal. Calcd for **1**: C 13.97, H 0.88, N 9.77. Found: C 14.08, H 0.95, N 9.68%. IR (ITR mode, cm^{-1}): 3441 (w), 3129 (s), 1612 (s), 1503 (s), 1450 (s), 1062 (s), 957 (s), 876 (s), 797 (s).

Photocatalysis. The photodegradation of Rhodamine-B (RhB) is investigated as model reaction to determine the photocatalytic activity of as-synthesized **1** and comparable samples under visible light irradiation. In the typical process, 25 mg of compound **1** (or AgCl, $(NBu_4)_4\{PW_{12}O_{40}\}$) was mixed together with 100 mL of 1.0×10^{-5} mol L^{-1} RhB solution in a 150 mL glass beaker by ultrasonic dispersion for 10 min. The mixture was stirred for 0.5 h to arrive at the surface-adsorption equilibrium of **1** under the darkness. Three milliliters of the sample was taken out from the glass beaker as the initial RhB concentration (C_0). The mixture was stirred continuously under visible light irradiation by using a 300 W high pressure Xe lamp. The distance of lamp to the glass beaker is ∼15 cm. Three milliliters of the samples were taken out from the glass beaker at certain irradiation time intervals. After centrifugations at 8000 rpm for 5 min to completely remove the powder of compound **1**, a clear solution was obtained. The UV−vis spectrophotometer was used to monitor the photodecomposition of RhB at 553 nm. The photocatalytic decomposition rate was defined as $1 - C/C_0$.

Antibacterial Testing. The *Escherichia coli* was chosen as model microorganism to investigate the antibacterial activity of **1**. Filter paper slices with the same size (1 cm) were selected as carriers to absorb **1** (or $(NBu_4)_4\{PW_{12}O_{40}\}$) and also to control samples. The suspensions of the samples with the concentration of 5 mg/mL were obtained by ultrasonic dispersion in deionized water for 10 min. Filter paper slices were dipped into the suspensions (or deionized water for blank experiments) several times for 1 min and dried. Luria−Bertani (LB) agar plates consisting of 1% of tryptone, 0.5% of yeast extract, 1% of sodium chloride, and 2% of agar were sterilized at 121 °C for ∼20 min and then to put into a Petri dish with ∼3 mm of thickness. A 0.2 mL aliquot of diluted bacterial suspension of *E. coli* was taken to spread on the surface of the nutrient LB agar uniformly. After 30 min, the as-prepared filter paper slices containing tested samples were placed on the Petri dish and incubated at 37 °C for ∼12 h. The diameters of zone inhibition were measured with calipers, and the results were recorded by camera.

X-ray Crystallography. A suitable single crystal of compound **1** was selected for single-crystal XRD analysis. The data were collected on a Bruker AXS SMART APEX II diffractometer in the range of 1.20−26.12° at the temperature of 293(2) K using graphite-monochromated Mo Kα radiation (λ = 0.710 73 Å). Data processing was accomplished with the SAINT processing program.[8] A total of 44 199 reflections were collected, of which 9199 reflections were unique. The structure of compound **1** was solved by direct method and refined by full matrix least-squares technique with the SHELXTL 97 crystallographic software package.[9] All non-H atoms were located from a difference Fourier map and refined anisotropically. All the H atoms of **L** ligands were added geometrically. Hydrogen atoms were not found on those solvent water molecules and, therefore, were not included in the final structure. The crystal data and structure refinement details of **1** are given in Table 1. Selected bond lengths and angles are given in Supporting Information, Table S1.

Table 1. Crystal Data and Structure Refinement for Compound 1

empirical formula	$C_{120}H_{144}Ag_{13}N_{72}O_{190}P_4W_{48}$
M	15 986.06
crystal system	trigonal
space group	$R\bar{3}$
a/ Å	21.6944(4)
b/ Å	21.6944(4)
c/ Å	51.068(2)
γ/ deg	120
V/ Å^3	20 814.9(10)
Z	3
D_c/ g cm^{-3}	3.826
μ(Mo Kα)/ mm^{-1}	20.832
max. and min. transmission	0.7453, 0.5053
F(000)	21 333
crystal size	0.35 × 0.2 × 0.20 mm
θ/ deg	1.20−26.12
data/params	9199/672
obsd reflns	44 199
goodness-of-fit on F^2	1.013
R_1, $wR_2{}^a$ [$I > 2\sigma(I)$]	0.0283, 0.0922
R_1, wR_2 (all data)	0.0386, 0.1025

$^aR_1 = \sum||F_0| - |F_c||/\sum|F_0|$, $wR_2 = \{\sum[w(F_0^2 - F_c^2)^2]/\sum[w(F_0^2)^2]\}^{1/2}$.

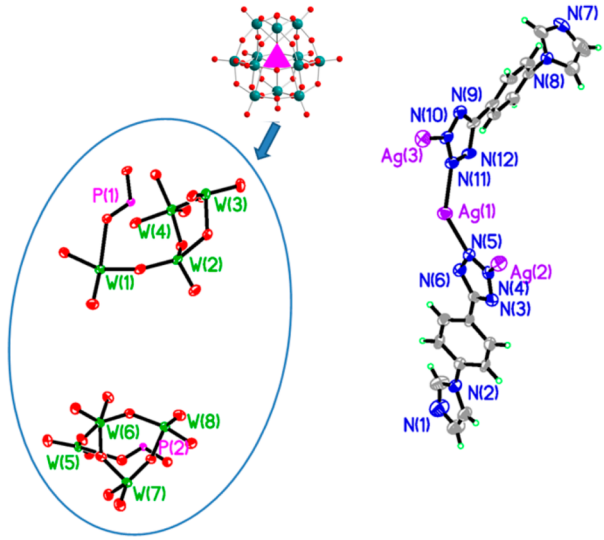

Figure 1. Asymmetric unit of the **1** showing the atomic labeling scheme. Atomic displacement ellipsoids are drawn at the 50% probability level. (inset) The used $\{PW_{12}O_{40}\}$ cluster. PO_4 is shown in the tetrahedron mode. Uncoordinated water molecules were omitted for clarity.

RESULTS AND DISCUSSION

Crystal Structure of $\{Ag_{13}(L)_{12}\}\{PW_{12}O_{40}\}_4\cdot 30H_2O$ (1). Single-crystal XRD analyses indicate that **1** crystallizes in trigonal crystal system with $R\bar{3}$ space group, with an asymmetric unit that contains three crystallographic independent Ag(I) ions, two noncoordinated $\{PW_{12}O_{40}\}^{3-}$ anions located on the 3-fold axis, two partly coordinated **L** ligands, and five water molecules (Figure 1). Each crystallographically independent Ag(2) ion lies on the 3-fold axis. The $PW_{12}O_{40}{}^{3-}$ anion is one of the most representative Keggin-type POM, which is composed by 12 WO_6 octahedra surrounding the central PO_4 tetrahedron. Three types of coordination environments in Ag centers have been observed within this $\{Ag_{13}L_{12}\}$ cluster (Figure 2a−c). Ag(1) is three-coordinated by nitrogen atoms from tetrazole moiety of **L** ligands to form a distorted trigonal $\{AgN_3\}$ geometry with Ag−N bond lengths ranging from

dx.doi.org/10.1021/ic501657p | Inorg. Chem. 2014, 53, 11584−11588

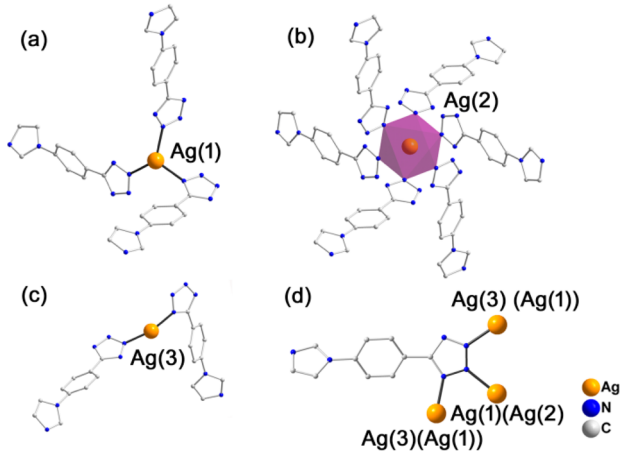

Figure 2. Three kinds of Ag environments (a–c) and the connection mode of **L** ligand (d) within **1**. Hydrogen atoms were omitted for clarity.

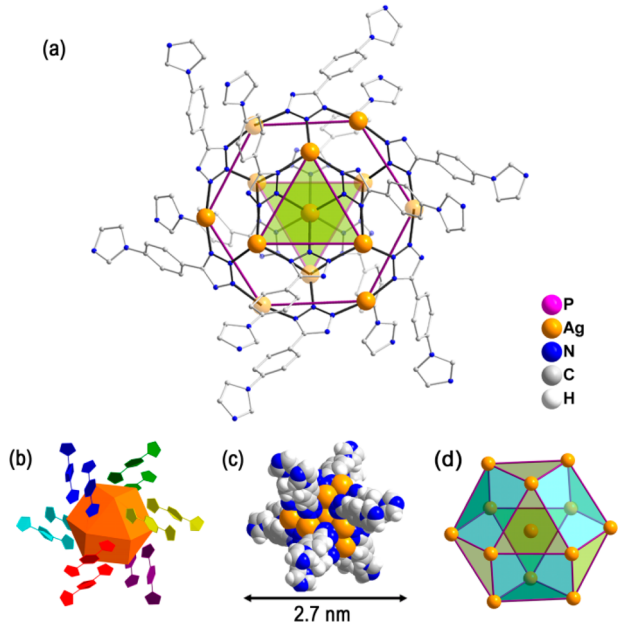

Figure 3. (a) The molecular structure of the $\{Ag_{13}L_{12}\}$ cluster within compound **1**, with the $\{Ag_{13}(N_3)_{12}\}$ core highlighted under thick black lines. (b) The structural view of the molecular windmill simplified from the $\{Ag_{13}L_{12}\}$ cluster. (c) The structural view of the $\{Ag_{13}L_{12}\}$ cluster using the packing representation. (d) The metallic skeleton of the $\{Ag_{13}L_{12}\}$ cluster with$\{Ag@Ag_{12}\}$-type cuboctahedral topology.

2.251(8) to 2.282(8) Å. Ag(2) locates in the central position of the whole cluster and is coordinated by six nitrogen atoms from the ligands, resulting a $\{AgN_6\}$ octahedron located on the 3-fold axis with the same Ag(2)–N bond lengths of 2.579(9) Å. The N–Ag–N angles between two adjacent N atoms are 81.7(2) and 98.3(2)°, respectively. Ag(3) adopts a nearly linear $\{AgN_2\}$ coordination geometry with N–Ag–N bond angle of 164.8(3) °. The Ag–N bond lengths of Ag(3) are ranging from 2.128(8) to 2.133(8) Å. All of the **L** ligands in $\{Ag_{13}L_{12}\}$ cluster utilize tetrazole functions partly coordinated to three Ag centers (Figure 2d).

The main structural motif within **1** is the nanosized $\{Ag_{13}L_{12}\}$ cluster with the diameter ca. 2.7 nm shows an intriguing molecular windmill shape. As illustrated in Figure

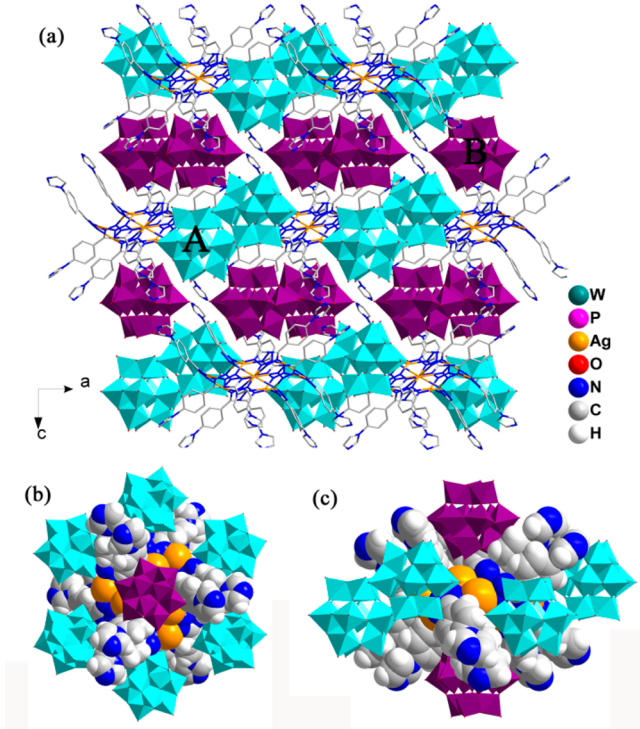

Figure 4. (a) View of the crystal structure of compound **1** along the *b*-axis. Hydrogen atoms were omitted for clarity. (b, c) The structural $\{Ag_{13}L_{12}\}$ cluster within **1**. The $\{Ag_{13}L_{12}\}$ clusters and POMs are given in the space-filling mode and polyhedral mode with the color of cyan (A) and pink (B) for clarity.

3a–c, the molecular windmill-shaped $\{Ag_{13}L_{12}\}$ cluster contains $\{Ag_{13}(N_3)_{12}\}$ core structure, which is composed by 13 Ag centers and 12 μ_3-bridging multidentate **L** ligands. Six pairs of **L** ligands can be considered as blades of this molecular windmill, while the central $\{Ag_{13}(N_3)_{12}\}$ core forms the axis. Another intriguing feature of the $\{Ag_{13}L_{12}\}$ cluster is its novel metallic skeleton (Figure 3d), in which 12 Ag ions surround the central Ag ion to construct a $\{Ag@Ag_{12}\}$-type core–shell structure with the cuboctahedral topology. The formed $\{Ag@Ag_{12}\}$ cuboctahedron consists of two {Ag(1)–Ag(1)–Ag(1)} triangular faces, six {Ag(1)–Ag(3)–Ag(3)} triangular faces, and six {Ag(1)–Ag(1)–Ag(3)–Ag(3)} rectangular faces with the Ag···Ag separations ranging from 3.579 to 6.133 Å, which is larger than the van der Waals radius of silver (3.44 Å). Although this cuboctahedral topology has already been found in many supramolecular architectures[10] and metal clusters[11] or some building blocks in metal–organic framework materials,[12] the $\{M@M_{12}\}$-type cuboctahedron has only been found in some metal crystals with metal–metal interactions, such as $\{Pt_{15}H_x(CO)_8(P^tBu_3)_6\}$ cluster containing centered cuboctahedral $\{Pt_{13}\}$ core caped by two $Pt(p\text{-}CO)_2(P^tBu_3)$ groups[13a] and a ferrocene-protected $\{Ag_{13}\}$ cluster.[13b] Hence, compound **1** represents the first polynuclear coordination complex with $\{M@M_{12}\}$-type cuboctahedral topology to the best of our knowledge.

The $\{Ag_{13}L_{12}\}$ cluster within **1** adopts hexagonal close-packed (HCP) mode stacking together along the *b* axis to construct supramolecular framework with 58% accessible void without considering the located POMs anions and water molecules, as calculated by PLATON software (Supporting Information, Figure S1).[14] Two types of cavities, namely, A and B, are filled by corresponding POMs templates (labeled by

dx.doi.org/10.1021/ic501657p | *Inorg. Chem.* 2014, 53, 11584–11588

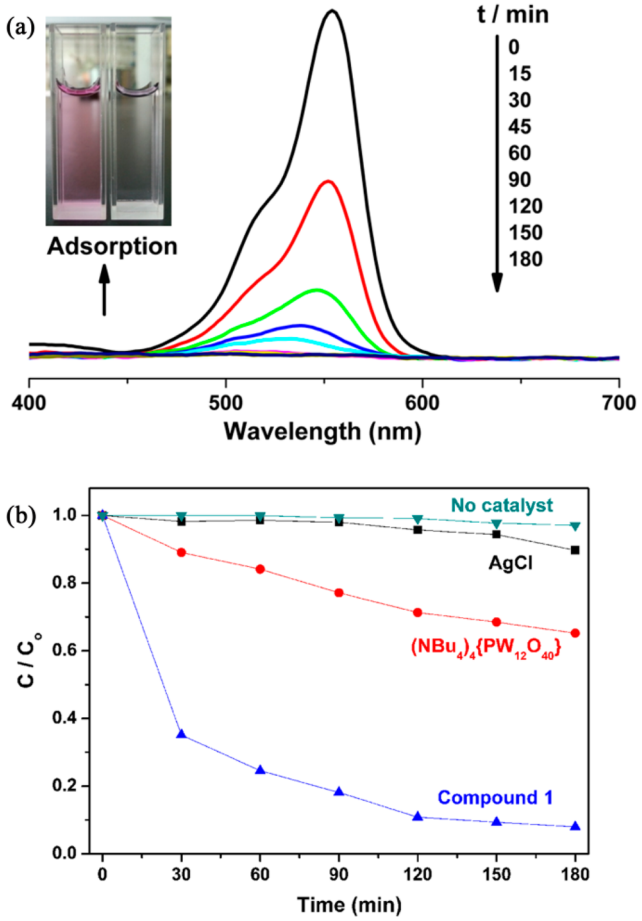

Figure 5. (a) Absorption spectra of the RhB solution during the photocatalytic decomposition reaction under visible light irradiation with the use of **1** (λ_{max} = 553 nm). (inset) Optical photograph of RhB solutions at 0 and 180 min. (b) The curves of RhB concentration versus irradiation time in the range of 0 to 180 min with the use of AgCl (black), $(NBu_4)_4\{PW_{12}O_{40}\}$ (red), **1** (blue), and blank (teal) under the same reaction condition.

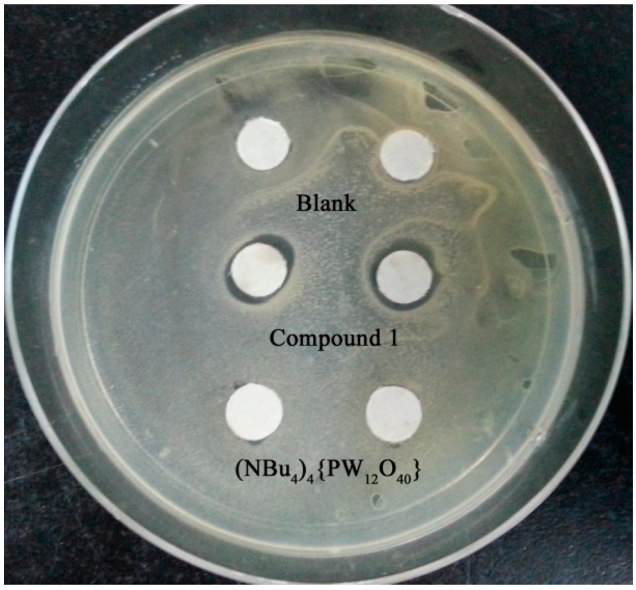

Figure 6. Optical photograph of antibacterial tests of **1**, with $(NBu_4)_4\{PW_{12}O_{40}\}$ and nothing added.

Table 2. Antibacterial Zones for 1 and the Contrastive Samples

sample	width of the antibacterial *E. coli* zone/ mm		
	d_{short}	d_{long}	$d_{average}$
1	0.8	4.1	2.5
1	2.5	3.3	2.9
$(NBu_4)_4\{PW_{12}O_{40}\}$	0	0.8	0.4
$(NBu_4)_4\{PW_{12}O_{40}\}$	0	0.6	0.3

different colors shown in Figure 4a). Each $\{Ag_{13}\mathbf{L}_{12}\}$ cluster surrounds eight POMs anions including six A-type POMs at the interspaces of neighboring windmill blades and two B -type POMs in the front faces of the molecular windmill (Figure 4b,c).

The Photocatalytic Activity of Compound 1. Considering the fact that both Ag complex[15] and POMs[16] can act as effective catalysts in various photocatalytic reactions, the photodegradation of Rhodamine-B (RhB) was chosen as a model reaction to examine the photocatalytic activity of as-synthesized **1** under the visible light irradiation. Moreover, the control experiments were carried out (a) using AgCl and $(NBu_4)_4\{PW_{12}O_{40}\}$ as catalysts and (b) without any catalyst under the same conditions. During irradiation, gradually hypsochromic shifts of the maximum absorption peaks of RhB solutions were observed in the presence of $(NBu_4)_4\{PW_{12}O_{40}\}$ as catalyst (Supporting Information, Figure S6). This phenomenon is observed in many catalytic systems, which is attributed to the N-deethylation of RhB to form some derivatives, such as *N,N,N′*-triethyl rhodamine and *N,N′*-diethyl rhodamine.[17] By contrast, the absorption peak of the RhB solution (553 nm) decreases largely using **1** as catalyst, while the hypsochromic shifts are considerably insignificant (Figure 5a). Furthermore, the irradiation time dependence of RhB concentrations was plotted up to 180 min of irradiation (Figure 5b). **1** exhibits the highest RhB degradation rate (nearly 90%) in contrast with AgCl (12%) and $(NBu_4)_4\{PW_{12}O_{40}\}$ (35%) after 180 min of irradiation. Moreover, the framework of compound **1** retains well after photocatalysis as proven in the powder XRD (Supporting Information, Figure S2). The combination of silver centers and $\{PW_{12}O_{40}\}^{3-}$ anions in the same framework seems to introduce a synergistic effect in improving the performance of photodegradation of RhB.[18]

The Antibacterial Activity of Compound 1. Another intriguing application of Ag complexes is as antibacterial agents used in the field of chemotherapy.[19] Hence, the antibacterial test against *E. coli* was investigated. As illustrated in Figure 6, around the filter paper slices carrying **1**, the areas of inhibition against the bacteria are obvious, and the antibacterial zones for **1** are measured and listed in Table 2. To determine the source of this antibacterial behavior, various control tests were performed. Scarcely any inhibition against *E. coli* bacterial activity was found in the filter paper slice carrying $(NBu_4)_4\{PW_{12}O_{40}\}$. The antibacterial activity of **1** is mainly ascribed to the Ag component. Moreover, the poor solubility of this compound makes it potentially useful as a solid antibacterial agent.

CONCLUSIONS

In summary, a nanosized molecular windmill-shaped polynuclear Ag cluster with the intriguing $\{M@M_{12}\}$-type cuboctahedral topology has been synthesized by using the POMs anion as template for the first time. Moreover,

dx.doi.org/10.1021/ic501657p | Inorg. Chem. 2014, 53, 11584−11588

compound **1** exhibits effective photocatalytic activity in degradation of RhB under visible light irradiation and also antibacterial activities against *E. coli*. The successful preparation of **1** proves that the "template-directing approach" is an effective method not only to form high-nuclearity metal clusters, but also to obtain novel hybrids with synergetic functions.

■ ASSOCIATED CONTENT

Supporting Information

Selected bond lengths and angles of compound **1**, structural views showing accessible void within compound **1**, powder XRD data, thermogravimetric analysis, infrared spectrum, and UV-vis spectrum of compound **1** and other catalysts. Crystal data in CIF format. This material is available free of charge via the Internet at http://pubs.acs.org. CCDC 1005585 with the supplementary crystallographic data for compound **1** can be obtained free of charge from the Cambridge Crystallographic Data Center via http://www.ccdc.cam.ac.uk/data_request/cif.

■ AUTHOR INFORMATION

Corresponding Authors

*E-mail: szm@ciac.ac.cn. Webpage: http://zhongmingsun.weebly.com/. (Z.M.S.)

*E-mail: xiez@ciac.ac.cn. (Z.X.)

Notes

The authors declare no competing financial interest.

■ ACKNOWLEDGMENTS

We thank the support of this work by National Nature Science Foundation of China (Nos. 21171162 and 21401188), Jilin Province Youth Foundation (20130522132JH), SRF for ROCS (State Education Ministry).

■ REFERENCES

(1) (a) Yam, V. W.-W.; Lo, K. K.-W.; Fung, W. K.-M.; Wang, C.-R. *Coord. Chem. Rev.* **1998**, *171*, 17−41. (b) Li, G.; Lei, Z.; Wang, Q.-M. *J. Am. Chem. Soc.* **2010**, *132*, 17678−17679. (c) Kikukawa, Y.; Kuroda, Y.; Yamaguchi, K.; Mizuno, N. *Angew. Chem., Int. Ed.* **2012**, *51*, 2434−2437. (d) Marambio-Jones, C.; Hoek, E. M. V. *J. Nanopart. Res.* **2010**, *12*, 1531. (e) Ray, S.; Mohan, R.; Singh, J. K.; Samantaray, M. K.; Shaikh, M. M.; Panda, D.; Ghosh, P. *J. Am. Chem. Soc.* **2007**, *129*, 15042−15053.

(2) (a) Rawashdeh-Omary, M. A.; Rashdan, M. D.; Dharanipathi, S.; Elbjeirami, O.; Ramesh, P.; Dias, H. V. *Chem. Commun.* **2011**, *47*, 1160−1162. (b) Jin, J.; Wang, W.; Liu, Y.; Hou, H.; Fan, Y. *Chem. Commun.* **2011**, *47*, 7461−7463. (c) Shimizu, G. K. H.; Enright, G. D.; Ratcliffe, C. I.; Preston, K. F.; Reid, J. L.; Ripmeester, J. A. *Chem. Commun.* **1999**, 1485−1486. (d) Dolomanov, O. V.; Blake, A. J.; Champness, N. R.; Schröder, M.; Wilson, C. *Chem. Commun.* **2003**, 682−683. (e) Sun, D.; Luo, G. G.; Zhang, N.; Huang, R. B.; Zheng, L. S. *Chem. Commun.* **2011**, *47*, 1461−1463. (f) Dias, H. V.; Diyabalanage, H. V.; Gamage, C. S. *Chem. Commun.* **2005**, 1619−1621. (g) Zhou, Y.; Chen, W.; Wang, D. *Dalton Trans.* **2008**, 1444−1453. (h) Chen, S.-C.; Yu, R.-M.; Zhao, Z.-G.; Chen, S.-M.; Zhang, Q.-S.; Wu, X.-Y.; Wang, F.; Lu, C.-Z. *Cryst. Growth Des.* **2010**, *10*, 1155−1160. (i) Hau, S. C.; Cheng, P. S.; Mak, T. C. *J. Am. Chem. Soc.* **2012**, *134*, 2922−2925. (j) Dias, H. V. R.; Gamage, C. S. P.; Keltner, J.; Diyabalanage, H. V. K.; Omari, I.; Eyobo, Y.; Dias, N. R.; Roehr, N.; McKinney, L.; Poth, T. *Inorg. Chem.* **2007**, *46*, 2979−2987.

(3) (a) Baxter, P. N. W.; Lehn, J.-M.; Baum, G.; Fenske, D. *Chem.—Eur. J.* **2000**, *6*, 4510−4517. (b) Hou, H.; Wei, Y.; Song, Y.; Mi, L.; Tang, M.; Li, L.; Fan, Y. *Angew. Chem., Int. Ed.* **2005**, *44*, 6067−6074. (c) Henkelis, J. J.; Kilner, C. A.; Halcrow, M. A. *Chem. Commun.* **2011**, *47*, 5187−5189.

(4) (a) Rais, D.; Yau, J.; Mingos, D. M. P.; Vilar, R.; White, A. J. P.; Williams, D. J. *Angew. Chem., Int. Ed.* **2001**, *40*, 3464−3467. (b) Bian, S. D.; Wu, H. B.; Wang, Q. M. *Angew. Chem., Int. Ed.* **2009**, *48*, 5363−5365. (c) Sun, D.; Wang, H.; Lu, H. F.; Feng, S. Y.; Zhang, Z. W.; Sun, G. X.; Sun, D. F. *Dalton Trans.* **2013**, *42*, 6281−6284.

(5) (a) Long, D. L.; Tsunashima, R.; Cronin, L. *Angew. Chem., Int. Ed.* **2010**, *49*, 1736−1758. (b) Wang, L.; Yang, W.; Yi, F.-Y.; Wang, H.; Xie, Z.; Tang, J.; Sun, Z.-M. *Chem. Commun.* **2013**, *49*, 7911−7913.

(6) Gao, G.-G.; Cheng, P.-S.; Mak, T. C. W. *J. Am. Chem. Soc.* **2009**, *131*, 18257−18259.

(7) (a) Zhai, Q.-G.; Wu, X.-Y.; Chen, S.-M.; Zhao, Z.-G.; Lu, C.-Z. *Inorg. Chem.* **2007**, *46*, 5046−5058. (b) Wang, D.-D.; Peng, J.; Pang, H.-J.; Zhang, P.-P.; Wang, X.; Zhu, M.; Chen, Y.; Liu, M.-G.; Meng, C.-L. *Inorg. Chim. Acta* **2011**, *379*, 90−94.

(8) *SMART and SAINT software packages;* Siemens Analytical X-ray Instruments Inc.: Madison, WI, 1996.

(9) Sheldrick, G. M. *Acta Crystallogr., Sect. A: Found. Crystallogr.* **2008**, *64*, 112.

(10) (a) Al-Rasbi, N. K.; Tidmarsh, I. S.; Auurgent, S. P.; Adams, H.; Harding, L. P.; Ward, M. D. *J. Am. Chem. Soc.* **2008**, *130*, 11641−11649. (b) Ghosh, K.; Hu, J.; White, H. S.; Stang, P. J. *J. Am. Chem. Soc.* **2009**, *131*, 6695−6697.

(11) (a) Awaleh, M. O.; Badia, A.; Brisse, F. *Inorg. Chem.* **2007**, *46*, 3185−3191. (b) Liao, J. H.; Latouche, C.; Li, B.; Kahlal, S.; Saillard, J. Y.; Liu, C. W. *Inorg. Chem.* **2014**, *53*, 2260−2267.

(12) (a) Ke, Y.; Collins, D. J.; Zhou, H.-C. *Inorg. Chem.* **2005**, *44*, 4154−4156. (b) Zhang, X.-M.; Fang, R.-Q.; Wu, H.-S. *J. Am. Chem. Soc.* **2005**, *127*, 7670−7671.

(13) (a) Howard, J. A. K.; Spencer, J. L.; Turner, D. G. *Dalton Trans.* **1987**, 259−262. (b) Albano, V. G.; Grossi, L.; Longoni, G.; Monari, M.; Mulley, S.; Sironi, A. *J. Am. Chem. Soc.* **1992**, *114*, 5708−5713.

(14) Spek, A. L. *Acta Crystallogr.* **2009**, *D65*, 148.

(15) (a) Bi, Y.; Ouyang, S.; Umezawa, N.; Cao, J.; Ye, J. *J. Am. Chem. Soc.* **2011**, *133*, 6490−6492. (b) Gouveia, A. F.; Sczancoski, J. C.; Ferrer, M. M.; Lima, A. S.; Santos, M. R.; Li, M. S.; Santos, R. S.; Longo, E.; Cavalcante, L. S. *Inorg. Chem.* **2014**, *53*, 589−5599. (c) Marcinkowski, D.; Wałęsa-Chorab, M.; Patroniak, V.; Kubicki, M.; Kądziołka, G.; Michalkiewicz, B. *New J. Chem.* **2014**, *38*, 604−610.

(16) (a) Papaconstantinou, E. *Chem. Soc. Rev.* **1989**, *18*, 1. (b) Sivakumara, R.; Thomas, J.; Yoon, M. *J. Photochem. Photobiol., C* **2012**, *13*, 277−298.

(17) (a) Watanabe, T.; Takizawa, T.; Honda, K. J. *Phys. Chem.* **1977**, *81*, 1845. (b) Takizawa, T.; Watanabe, T.; Honda, K. J. *Phys. Chem.* **1978**, *82*, 1391.

(18) (a) Hu, Y.; Luo, F.; Dong, F. *Chem. Commun.* **2011**, *47*, 761−763. (b) Sha, J.; Li, M.; Sun, J.; Yan, P.; Li, G.; Zhang, L. *Chem.—Asian J.* **2013**, *8*, 2254−2261. (c) Li, M.-T.; Sha, J.-Q.; Zong, X.-M.; Sun, J.-W.; Yan, P.-F.; Li, L.; Yang, X.-N. *Cryst. Growth Des.* **2014**, *14*, 2794−2802.

(19) (a) Nomiya, K.; Takahashi, S.; Noguchi, R.; Nemoto, S.; Takayama, T.; Oda, M. *Inorg. Chem.* **2000**, *39*, 3301−3311. (b) Nomiya, K.; Takahashi, S.; Noguchi, R. *Dalton Trans.* **2000**, 2091−2097. (c) Abu-Youssef, M. A. M.; Dey, R.; Gohar, Y.; Massoud, A. a. A.; Öhrström, L.; Langer, V. *Inorg. Chem.* **2007**, *46*, 5893−5903. (d) Pettinari, C.; Marchetti, F.; Lupidi, G.; Quassinti, L.; Bramucci, M.; Petrelli, D.; Vitali, L. A.; da Silva, M. F.; Martins, L. M.; Smolenski, P.; Pombeiro, A. J. *Inorg. Chem.* **2011**, *50*, 11173−11183. (e) Massoud, A. A.; Langer, V.; Gohar, Y. M.; Abu-Youssef, M. A.; Janis, J.; Lindberg, G.; Hansson, K.; Ohrstrom, L. *Inorg. Chem.* **2013**, *52*, 4046−4060.